Results in Surfaces and Interfaces 19 (2025) 100524

Contents lists available at ScienceDirect

Results in Surfaces and Interfaces

journal homepage: www.elsevier.com/locate/rsurfi

Bimetallic AuAg-coated porous silicon nanowire platform for rapid SERS-based antibiotic susceptibility testing

Daria A. Nazarovskaia [a,*], Pavel A. Domnin [a,b], Oleg D. Gyuppenen [a], Ilia I. Tsiniaikin [a], Svetlana A. Ermolaeva [b], Kirill A. Gonchar [a], Liubov A. Osminkina [a,**]

[a] Faculty of Physics, Lomonosov Moscow State University, Moscow, 119991, Russian Federation
[b] Gamaleya Research Centre of Epidemiology and Microbiology, Moscow, 123098, Russian Federation

ARTICLE INFO

Keywords:
Porous silicon nanowires
Antibiotic susceptibility testing
Biosensors
Surface-enhanced Raman scattering
Antimicrobial resistance
Bacteria
Listeria innocua

ABSTRACT

Rapid antibiotic susceptibility testing (AST) is crucial for selecting appropriate antibiotic treatments and customizing empirical therapy to effectively manage serious bacterial infections. This study focuses on developing and characterizing surface-enhanced Raman scattering (SERS)-active nanostructured composite substrates designed for swift and highly sensitive bacterial detection, followed by accelerated AST. The substrates were fabricated by depositing noble metal nanoparticles (Au, Ag) onto porous silicon nanowires (pSiNWs) formed through metal-assisted chemical etching (MACE) of crystalline silicon. Scanning electron microscopy (SEM) images depict *Listeria innocua* bacteria localized in close proximity to AuAg nanoparticles atop pSiNWs. SERS spectra of *L.innocua* were acquired using a 633 nm laser beam, enabling rapid label-free bacterial detection. Comparisons with the traditional disk diffusion method show that the developed SERS approach allows for real-time monitoring of bacterial antibiotic susceptibility within 3 h, in contrast to the standard 24-h test duration. These findings underscore the potential of AuAg@pSiNWs substrates to expedite the AST process, offering a significant advantage in clinical diagnostics and antimicrobial resistance monitoring.

1. Introduction

The development of rapid and reliable methods for bacterial antibiotic susceptibility testing (AST) is relevant for healthcare and medicine. Indeed, today the greater number of bacteria is becoming resistant to various antibiotics, which leads to severe courses of infectious diseases that often have serious consequences for health and well-being of patients. Since the 2000s, the World Health Organization has identified antibiotic resistance as one of the most serious threats to human health [1]. AST is used to help find the best treatment for a bacterial infection [2]. For a long period of time, phenotypic methods, such as disk diffusion, gradient diffusion or agar dilution, have been gold standards for AST [3]. In general, these methods are based on the isolation of bacteria in pure culture, its identification, the exposure of isolates to a set of antibiotics and subsequent visual detection. These traditional approaches are time-consuming, taking 18–72 h to get a result, which is critical in cases of life-threatening infections such as sepsis, salmonella, pneumonia, meningitis and others, where a delay in treatment can lead to severe complications. Apart from that, additional drawbacks of phenotypic methods include poor test performance for slow-growing bacteria, sensitivity to the maintenance of pH, temperature, nutrition media, etc [4]. Fortunately, many novel methods and tools offer AST in minutes or in few hours using non-purified polymicrobial samples, that, according to their principle, can be 1) the detection of genes related to AR (Nucleic Acid Amplification Technology (NAAT)), 2) nucleic acid hybridization-based techniques (Fluorescence In Situ Hybridization (FISH)), 3) biosensing [5].

Over the past decade, much effort has been devoted to the development of new biosensors for the rapid detection of bacteria, and optical biosensors have been widely studied [6]. These biosensors detect the presence of molecules based on the utilization of light by monitoring changes in absorption, reflection, transmission or emission of the biosensor, and they offer advantages such as speed, selectivity, sensitivity and reproducibility. To date, advances in biosensor technology have led to promising results; however, sensitive real-time detection of bacteria in the clinic has yet to be realized. The main limitations are

* Corresponding author.
** Corresponding author.
E-mail addresses: nazarovskaia.da22@physics.msu.ru (D.A. Nazarovskaia), osminkina@physics.msu.ru (L.A. Osminkina).

https://doi.org/10.1016/j.rsurfi.2025.100524
Received 25 November 2024; Received in revised form 24 March 2025; Accepted 10 April 2025
Available online 18 April 2025

related to the lack of sensitivity to low bacterial load without the use of amplification or sample enrichment, and the inability to meet stringent clinical requirements [7].

Spectroscopic techniques based on the vibrational transitions of molecules draw special attention and supply precise spectral information in the form of distinctive fingerprint-like patterns that are specific to individual molecular structures. Surface-enhanced Raman spectroscopy (SERS) emerges as a promising avenue, offering the advantages of ultrasensitive and non-destructive biomedical analysis [8]. In SERS, molecules experience a highly localized and significantly amplified electromagnetic field at the surface of metal nanostructures when the excitation wavelength resonates with localized surface plasmons. This resonance leads to a substantial increase in Raman scattering intensity, enabling the detection of even single molecules. The enhancement primarily arises from electromagnetic effects, where intense field confinement in nanostructured "hot spots" boosts the signal by factors of 10^8 - 10^{12}, and chemical effects, which involve charge transfer interactions modifying molecular polarizability. The efficiency of SERS depends on the nanostructure geometry, metal composition, and analyte proximity, making it a powerful tool for ultrasensitive molecular detection and biosensing [9,10].

Porous silicon (pSi) as well as silicon nanowires (SiNWs) substrates decorated with noble metal nanoparticles are rapidly finding applications in SERS technology [11,12], which may enable new systems for bacterial and AST detection. It is well-known that silicon nanostructures are an excellent template for the formation of plasmonic nanostructures whose morphology can be tuned by the initial nanostructured silicon substrate [13]. The tunable shape and size of the metal particles, as well as the spacing between them, in turn contribute to the surface plasmon resonance effect, which, being perfectly matched to the excitation wavelength, helps to achieve the strongest possible SERS signal [14,15]. Recently, Muthukumar and Shtenberg presented a SERS-active platform made of silver-embed pSi thin films functionalized with either 4-aminothiphenol Raman tag [16] or aptamer complex [17] that achieves high sensitivity on the order of 10^1 CFU/mL in the detection of harmful bacteria from real-life samples (raw milk taken from different animals, ground water, fish). The reported biosensors rely on the indirect approach of detection, whereas a label-free technique is based on the direct interaction of the bacteria with a SERS substrate and may have significant benefit over label-based methodology. Given the highly developed and precisely adjustable structure and pore size, pSi may well accommodate individual bacterial cells on its surface, promoting simple SERS detection of microorganisms without the need for additional labels. For instance, in the work [18], label-free Ag -coated pSi SERS chips were used for the investigation of three *Escherichia coli (E. coli)* resistive and suspectable strains. It has been shown that more bacterial resistances are reflected in more of their Raman peaks; thus, with the addition of a neural network, it is possible to obtain and differentiate SERS profiles of different pathogens for clinical bacterial diagnosis in the future. For better SERS properties, bimetallic plasmonic nanoparticles layers can be grown on pSi, as shown in [19], where bacterial monitoring was performed using pSi gradient pore nanostructures with the alloys of composite Ag and palladium (Pd) nanoparticles prepared inside the porous network. The value of the enhancement factor was about $2\bullet10^5$, offering an efficient way the detection of ultralow bacterial concentrations as low as 1 CFU/mL.

SiNWs with a bimetallic AuAg coating have demonstrated significant advantages over monometallic gold or silver coatings for SERS analysis. The combination of Ag and Au provides a synergistic enhancement effect, where silver ensures strong electromagnetic field amplification, while gold enhances chemical stability and biocompatibility of the nanostructure. Additionally, bimetallic coatings enable flexible tuning of plasmonic properties, improving the sensitivity and reproducibility of SERS spectra [20]. Previously, we proposed the use of Ag- and/or Au-coated pSiNWs for SERS diagnostics of pyocyanin, a specific metabolite of *Pseudomonas aeruginosa*, marking the first report on SERS-based direct detection of this biomarker in complex biological media such as sputum [20]. Subsequently, stable SERS signals were achieved for bilirubin detection, with an impressive detection limit of 1 μM on Au-modified SiNWs [21]. Furthermore, these SERS-active structures were successfully applied for the detection of internalin B, a protein associated with the pathogenic bacterium *Listeria monocytogenes* [22]. In our latest work, we fabricated AuAg@pSiNWs and explored their application in label-free SERS bacterial analysis [23]. The resulting SERS sensor exhibited a limit of detection (LOD) of 10^4 CFU/mL for *L. innocua*, demonstrating its potential for sensitive bacterial detection.

In the present work, we investigate the use of AuAg-coated porous silicon nanowires as a SERS-active platform for the rapid detection of *L. innocua* and real-time antibiotic susceptibility testing. We demonstrate that AuAg@pSiNWs enable the acquisition of highly reproducible SERS spectra of *L.innocua*, with characteristic Raman bands reflecting bacterial cell wall components and metabolic products. Furthermore, SERS-based AST revealed distinct spectral changes in response to benzylpenicillin and gentamicin treatment, correlating with bacterial susceptibility, while no significant spectral variations were observed for streptomycin, confirming bacterial resistance. Compared to conventional disk diffusion tests, which require 24 h, the SERS-based approach provided conclusive results within 3 h. These findings underscore the potential of AuAg@pSiNWs as a highly sensitive and rapid diagnostic tool for bacterial detection and AST, with the possibility of future adaptation for a broader range of bacterial pathogens.

2. Materials and methods

2.1. Materials

Heavily boron-doped (100)-oriented crystalline silicon wafers with the resistivity of 1–5 mΩ cm (Telekom-STV, Russia), hydrofluoric acid (chemically pure) 45 % (Sigma Tech, Russia), hydrogen peroxide solution 30 % (w/w) in H_2O (Sigma-Aldrich, USA), Gold(III) chloride 99.9 % (metals basis) (ABCR, Germany), silver nitrate, 99+% (Alfa Aesar, USA), brain heart infusion broth (Becton Dickinson, USA), phosphate-buffer saline (Sigma-Aldrich, USA), streptomycin (Sigma Aldrich, USA), gentamicin (Sigma Aldrich, USA) and benzylpenicillin (Sigma Aldrich, USA).

2.2. Fabrication of AuAg@pSiNWs SERS-active substrates

The porous silicon nanowire (pSiNW) arrays were prepared by metal-assisted chemical etching (MACE) of the crystalline silicon (c-Si) wafer, wherein gold nanoparticles (Au NPs) initiated the nanowire growth. Before etching, the c-Si wafer was cleaned in acetone and isopropanol in an ultrasonic bath (Elmasonic S, Germany) for 2 min in each solvent to remove accidental organic and inorganic residues, and in 5 M HF (aqueous solution) for 5 min to dissolve an oxide film formed during the storage of c-Si wafers in air.

A schematic representation of the preparation of AuAg@pSiNWs is shown in Fig. 1. In the first step of MACE, Au NPs were deposited on the surface of c-Si by immersing the purified c-Si in a solution consisting of 5 M HF and 0.01 M $AuCl_3$ (*v:v* 1:1) for 15 s. After coating with Au NPs, the c-Si wafer was immersed in a second solution consisting of 5 M HF and 30 % H_2O_2 (v:v 10:1) for 8 min. Au NPs act as catalysts, locally oxidizing the silicon surface and facilitating directional etching, resulting in the formation of vertically aligned pSiNWs, with Au NPs remaining at their base, as illustrated in Fig. 1. The freshly etched pSiNW arrays were then decorated with noble metal particles (Ag, Au) by sequentially immersing them in 0.02 M $AgNO_3$ and 0.01 M $AuCl_3$ aqueous solutions for 30 s each. The process was stopped by immersing the sample in DI water. The obtained AuAg@pSiNWs were dried at room temperature (RT) and then cut into 0.5 × 0.5 cm^2 chips.

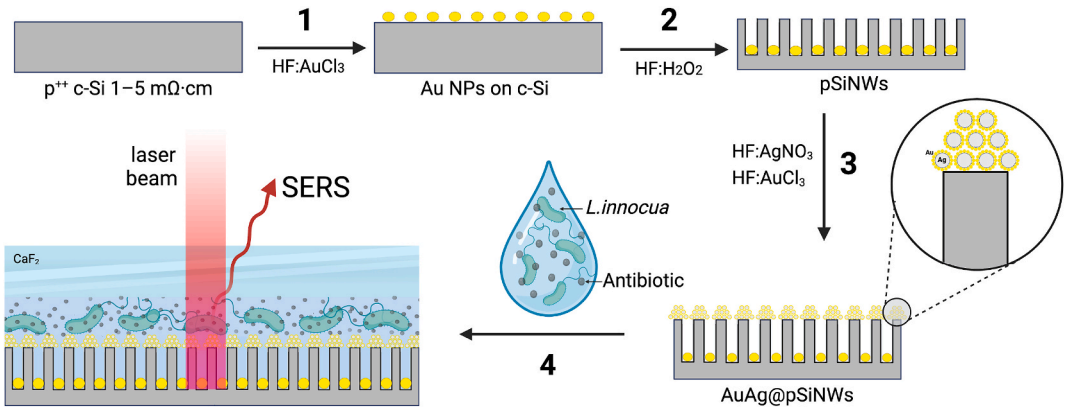

Fig. 1. Schematic representation of AuAg@pSiNWs chip production for antibiotic susceptibility testing of bacteria by SERS method.

2.3. Bacteria strain and growth conditions

Listeria innocua (*L.innocua*) strain SLCC3379 was obtained from N. F. Gamaleya National Research Center for Epidemiology and Microbiology (Russia) and maintained at −70 °C in 10-% glycerol. The bacteria were cultivated overnight in the brain heart infusion (BHI) broth at 37°C under constant shaking at 180 rpm. Then, it was diluted 1:100 with the fresh medium to obtain the concentration of $3.2\bullet10^7$ CFU/mL (colony-forming unit per mL).

2.4. Scanning electron microscopy

Scanning electron microscopy (SEM) studies of AuAg@pSiNWs before and after SERS experiments were undertaken with Carl Zeiss SUPRA 40 field emission – scanning electron microscope (Carl Zeiss, Germany) at an accelerating voltage of 2 keV. *L.innocua* were immobilized on the AuAg@pSiNWs surface using a 2.5 % glutaraldehyde solution in phosphate-buffer saline (PBS) for 90 min, and then dehydrated by the successive use of 50-% to absolute ethanol [24].

2.5. Energy-Dispersive X-ray spectroscopy

Energy-Dispersive X-ray Spectroscopy (EDX) analysis was conducted using a Supra 50VP FEG microscope equipped with an INCA X-Max80 X-ray detector. The acquired spectra were processed with Aztec software. Measurements were performed at an acceleration voltage of 5 keV, ensuring a spatial resolution of less than 100 nm for 90 % of the detected signal and approximately 300 nm for the full signal range.

2.6. Surface-enhanced Raman spectroscopy

To examine L.*innocua* by surface-enhanced Raman spectroscopy (SERS), bacteria were transferred by centrifugation in PBS, then 10 μL of bacterial suspension at a concentration of $3.2\bullet10^7$ CFU/mL was gently applied to the AuAg@pSiNWs chip and securely encapsulated in a custom-made sealed cell. The cell had a metal base and a lid made of CaF_2 optical window.

For antibiotic sensitivity testing, bacteria in the exponential growth phase were transferred to PBS ($3.2\bullet10^7$ CFU/mL in fresh PBS), then a PBS suspension of 0.5 mg/mL antibiotic was added in a 1:1 vol ratio. A 10 μL drop of the resulting mixture was applied to the AuAg@pSiNWs chip and placed in the custom-made cell for SERS analysis. The antibiotics used in the assay were streptomycin, gentamicin, and benzylpenicillin.

SERS spectra were acquired utilizing a Confotec MR350 Raman confocal microscope-spectrometer (SOL Instruments, Belarus), equipped with a Nikon Plan Fluor 10 × /0.30 microscope objective lens (Nikon Instruments, Japan). The sample was illuminated by a laser beam at an emission wavelength of 633 nm (diode laser 0 633L-21A, Integrated Optics, UAB, Lithuania), which was focused onto the sample with a spot size approximately 0.5 μm in diameter. The average laser excitation power was set at 2 mW (LaserCheck handheld power meter (Coherent, USA), and an accumulation time of 30 s was employed. Three spectra were recorded at each designated location and presented within the spectral range of 450–1750 cm^{-1}.

2.7. Disk diffusion antibiotics susceptibility test

Traditional disk diffusion antibiotic susceptibility testing (AST) was performed on 0.7 % agar plate. The stationary culture of *L.innocua* SLCC3379 ($3.2\bullet10^7$ CFU/mL) was diluted 1:100 with 4 mL of sterile liquid BHI 0.7 % agar and poured into the 90 mm Petri dish. After agar cooling, AuAg@pSiNWs were placed on agar surface as well as 10 μL of streptomycin, gentamicin and benzylpenicillin at the concentration of 30 μg/mL each. After 24-h of incubation at 37 °C zones of inhibitions were measured.

2.8. CFU count after antibiotic treatment in PBS

To determine changes in antibiotic resistance attributed to the PBS, gentamicin, benzylpenicillin and streptomycin were added to the bacterial culture suspended in PBS to a final concentration of 500 μg/mL. After 3 h, viable cells were determined by plating of serial dilutions of bacterial suspension on the BHI agar and CFU counting after 24 h of incubation at 37 °C.

3. Results and discussion

3.1. Scanning electron microscopy study and EDX analysis

Fig. 2 shows SEM micrographs of as-fabricated AuAg@pSiNWs (Fig. 2a and b) and after the immobilization of *L.innocua* bacteria onto its surface (Fig. 2 c). The cross-sectional SEM image (Fig. 2a) demonstrating a vertically aligned porous nanowire array oriented along the crystallographic direction [100], with a uniform height of approximately 2.2 μm, an average diameter of the nanowires ~ 50 nm. The resulting high-aspect-ratio pSiNWs exhibit a well-defined morphology, with Au NPs retained at their base post-etching. At the top of the nanowires, a bimetallic nanoparticle layer with a thickness ~400 nm is observed, ensuring a sufficiently dense metal coverage for optimal plasmonic enhancement while maintaining porosity for effective molecule adsorption.

Top-view SEM image of the AuAg@pSiNWs (Fig. 2b) revealing a highly interconnected porous nanostructure with a dense and uniform distribution of Ag and Au nanoparticles across the nanowire surface. The bright, evenly dispersed dots correspond to the noble metal

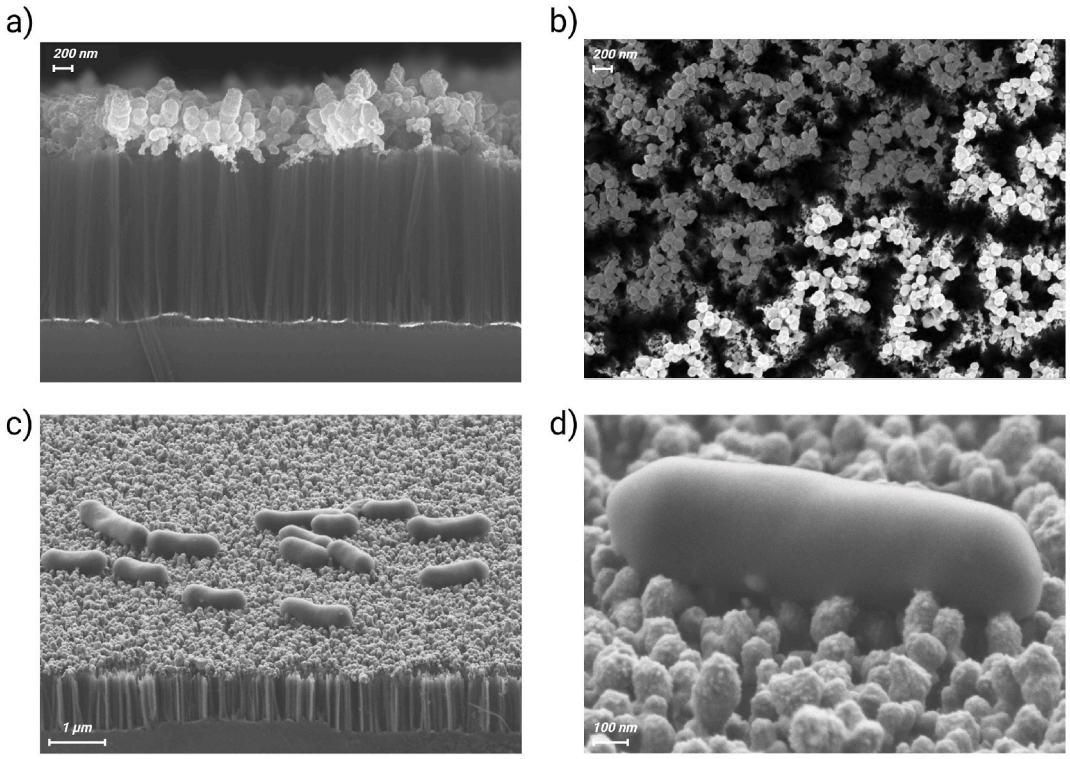

Fig. 2. SEM images of AuAg@pSiNWs: side view(a); top view(b), and AuAg@pSiNWs after incubation with *L.innocua* bacteria: tilted view (c); tilted view with magnification (d).

nanoparticles, confirming the successful metal deposition process. This uniform coverage facilitates the formation of plasmonic hot spots, which are crucial for surface-enhanced Raman spectroscopy (SERS) applications.

To determine the composition and spatial distribution of Au and Ag in the bimetallic system, we performed EDX analysis. The results indicate that gold is present at both the external and internal interfaces of the pSiNWs, whereas silver is predominantly localized at the external interface but also penetrates into the structure to some extent. This distribution is explained by the fabrication process: Au NPs initially serve as catalysts for nanowire formation via MACE, resulting in their incorporation at the bottom of the nanowires. Additionally, gold was used in a subsequent deposition step to coat the tops of the nanowires, leading to its presence at both interfaces. In contrast, silver was deposited in the final step, leading to its primary localization at the external surface, though some penetration into the porous network was also observed. The measured atomic ratio of Au to Ag at the external interface is approximately **3:1**, ensuring a stable and reproducible SERS signal. The full EDX spectra and depth profiles have been included in the Supplementary Information (SI) as Fig. S1.

Fig. 2c shows the immobilization of *L.innocua* bacteria on the surface of AuAg@pSiNWs. The bacterial cells exhibit the characteristic rod-shaped morphology of *Listeria innocua* and are evenly distributed across the nanostructured substrate. Their effective immobilization is facilitated by the high nanoscale roughness and porosity of pSiNWs, which provide an increased contact area and numerous active AuAg sites for subsequent SERS analysis.

Fig. 2d presents a high-magnification SEM image of an individual *L. innocua* cell on the AuAg@pSiNWs surface. The bacterium retains its typical rod-like shape, with a length of approximately 1 μm and a diameter of 500 nm. The bacterial surface remains morphologically intact, indicating no significant damage during the immobilization process.

3.2. Surface-enhanced Raman spectroscopy bacterial detection and AST analysis

Fig. 3 presents the Raman and SERS spectra of *L.innocua* ($3.2\bullet10^7$ CFU/mL) obtained using pSiNWs and AuAg@pSiNWs substrates, along with an evaluation of measurement reproducibility. Fig. 3a displays the mean Raman and SERS spectra, with the grey-shaded area indicating the standard deviation calculated from three independent measurements. The pSiNWs substrate without metal nanoparticles does not exhibit any significant enhancement of the Raman signal, with only the characteristic 520.5 cm^{-1} peak corresponding to the optical phonon mode of crystalline silicon being clearly observed [25]. In contrast, the SERS spectrum obtained on AuAg@pSiNWs reveals a set of highly intense and well-defined Raman peaks, forming a distinctive molecular fingerprint of *L.innocua*. The fluorescent background observed in the spectra arises from the intrinsic fluorescence of bacterial biomolecules and the silicon-based substrate, which contributes to the spectral baseline.

Fig. 3b illustrates the reproducibility of the SERS signal across different batches of substrates. Three independent SERS spectra were recorded from three different batches of AuAg@pSiNWs, demonstrating high batch-to-batch consistency. The concentration of bacteria in all measurements was $3.2\bullet10^7$ CFU/mL. Fig. 3c provides a comprehensive evaluation of the reproducibility of SERS spectra across multiple bacterial batches. Three independent SERS spectra were collected from three bacterial batches, each analyzed on three different substrate batches, yielding a total of nine data sets. The bacterial concentration remained constant at $3.2\bullet10^7$ CFU/mL. In both cases, the signal intensity was evaluated based on the maximum intensity of the characteristic SERS peak at 1320 cm^{-1}, which was consistently observed in all spectra. These results confirm the stability and reproducibility of the SERS-based detection method, highlighting its robustness for bacterial diagnostics.

The tentative assignments of the observed SERS of peaks of *L.innocua* are summarized in Table 1, which primarily reflect the vibrational modes of bacterial cell wall constituents, including membrane lipids,

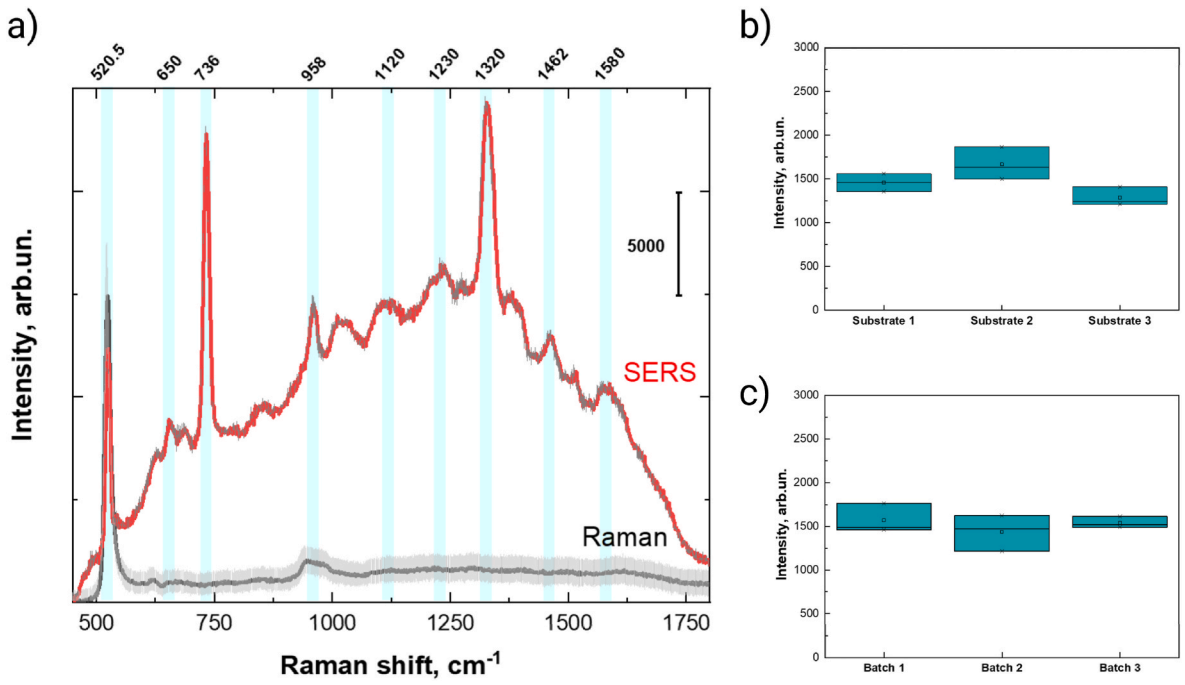

Fig. 3. Raman and SERS spectra of *L.innocua* ($3.2 \bullet 10^7$ CFU/mL) recorded on pSiNWs (black curve) and AuAg@pSiNWs (red curve) substrates, along with reproducibility assessment. (a) Mean Raman and SERS spectra of *L.innocua* with standard deviation (shaded region) based on three independent measurements. (b) Box plot representation of the SERS intensity distribution obtained from three different AuAg@pSiNWs substrate batches. (c) A box plot analysis of SERS intensity variations across three bacterial batches, each tested on three different substrate batches (nine data sets in total). The signal intensities in (b) and (c) were determined based on the maximum intensity of the SERS peak at 1320 cm^{-1}.

Table 1
Raman bands in the SERS spectrum of *L.innocua* adsorbed on AuAg@pSiNWs and their suggested assignments.

Raman band, cm^{-1}	Suggested assignment	Ref.
650	Guanine	[31,32]
736	Ring breathing mode of adenine and its nucleotides (AMP, ATP); glycosidic ring vibration of *N*-acetylglucosamine (NAG) in peptidoglycan	[26,27, 30]
950	The band assignment of given bacteria types around 925–940 cm− 1 is generally produced by membrane phospholipids.	[28]
1130	C–N and C–C stretch (carbohydrates)	[26,29]
1240	NH-bending in combination with C–N stretching in Amide III (proteins)	[26,28]
1320	CH_2-deformation in proteins or glutamine (Gln); possible contribution from adenine-related molecular vibrations	[27–30]
1462	CH_2-bending in Amide III	[30]
1580	NH-bending in combination with C–N stretching in Amide II (proteins)	[26,29, 30]

AMP: Adenosine monophosphate; ATP: Adenosine triphosphate; NAG: *N*-acetylglucosamine; Gln: Glutamine.

polysaccharides, proteins, amino acids, nucleic acids, and metabolites of purine breakdown. These are the components in direct contact with metal NPs, which primarily contribute to the SERS signal. Our results largely correspond to the characteristic SERS spectra of *Listeria* species reported in previous studies [26] but also exhibit some additional peaks that may be specific to the *L. innocua* SLCC3379 strain. Despite the widespread use of SERS in bacterial diagnostics, bacteria are biochemically complex objects, and the molecular origin of some Raman bands remains under discussion.

One possible explanation for the strong signal at 736 cm^{-1} is the ring breathing mode of adenine and its nucleotides (Adenosine monophosphate, AMP and Adenosine triphosphate, ATP), which are key components of nucleic acids and cellular metabolism in bacteria [27]. This band has also been associated with glycosidic ring vibrations of N-acetylglucosamine (NAG), a major structural component of peptidoglycan in Gram-positive bacterial cell walls [26]. Given the overlap of these assignments, the 736 cm^{-1} peak likely reflects a combination of contributions from both adenine-containing biomolecules and peptidoglycan. The 950 cm^{-1} peak is generally attributed to membrane phospholipids, as reported in SERS studies of bacterial species. This assignment aligns with the vibrational modes observed in lipid-rich bacterial membranes [28]. The 1130 cm^{-1} peak corresponds to C–N and C–C stretching vibrations found in carbohydrates. This band has been reported in bacterial SERS spectra, particularly in association with peptidoglycan and polysaccharide components of the bacterial cell wall [26,29].

The 1320 cm^{-1} peak was previously attributed to CH_2-deformation in proteins [30] or the presence of glutamine (Gln) within the bacterial cell wall [28]. However, given our comparison with SERS spectra of adenine, this peak may also include a contribution from adenine-related molecular vibrations, further supporting the role of nucleotides in the bacterial SERS signal [27]. Another essential part of bacterial DNA/RNA, guanine, has the characteristic SERS band at 650 cm^{-1} [31, 32]. Additionally, the characteristic SERS features of the bacterial cell wall include amide bands, which provide insights into the secondary structure of proteins. The 1240–1310 cm^{-1} range corresponds to Amide III vibrations (a combination of C–N stretching and N–H bending), while Amide II appears within 1550–1580 cm^{-1}, involving N–H bending and C–N stretching [30]. The 1462 cm^{-1} peak, assigned to CH_2-bending in Amide III, has been linked to protein structural changes and lipid interactions in bacterial cell walls. This peak may also reflect vibrations in complex phospholipid assemblies, which play a crucial role in bacterial membrane integrity [30]. These spectral features align well with previously reported SERS studies of Listeria species [26,29].

Having established the effectiveness of the SERS method for bacterial detection, we next applied it to antibiotic susceptibility testing (AST) to evaluate bacterial response to different antibiotics in real time.

Fig. 4a and Table 2 show the results of the disk diffusion test for the sensitivity of *L.innocua* to 3 different antibiotics: benzylpenicillin, gentamicin and streptomycin, and to AuAg@pSiNWs. It is seen that while the lawn of bacteria was not disrupted in the presence of streptomycin, its response to other drugs was visible. The diameters of inhibition zones of bacteria after 24-h incubation with benzylpenicillin and gentamicin were 15 mm and 7 mm, respectively. No bacterial growth inhibition was observed for AuAg@pSiNWs chips that were placed on agar with the nanostructures upper side (black side in photo) or down (grey side in photo). The number of CFU/mL after 3-h antibiotic treatment of *L.innocua* in PBS is shown in Fig. 4b. No antibiotics were added to the control group. The introduction of 500 μg/mL of benzylpenicillin or gentamicin to *L.innocua* exponential culture resuspended in PBS caused a 40-fold decrease in the number of CFU 3 h later. However, the introduction of streptomycin at the same concentration did not cause any significant changes which indicates higher resistance of the bacteria to this antibiotic.

To further explore the potential of SERS-based diagnostics, we investigated how the SERS spectra of *L.innocua* change under antibiotic treatment, allowing us to assess bacterial susceptibility in a rapid and label-free manner. Fig. 5 a, b, and c present the SERS spectra of *L.innocua* ($3.2 \bullet 10^7$ CFU/mL) treated with benzylpenicillin, gentamicin, and streptomycin solutions in PBS (500 μg/mL) for 0, 60, 120 and 180-min incubation period. According to the disk diffusion test presented above, the selected antibiotic concentration should effectively inhibit the susceptible bacteria. After background removal in the SERS spectra, the bacteria peaks at 736 and 1320 cm^{-1} were the most prominent, so the dependence of their Raman intensities on incubation time is shown separately (Fig. 5 d, e, f). Standard deviations were obtained from three individual measurements of the bacterial sample for each incubation time condition.

According to the results presented in Fig. 5, a significant decrease in the intensity of the Raman peaks for *L.innocua* treated with benzylpenicillin was observed: approximately 5-fold at 736 cm^{-1} and nearly 100 % at 1320 cm^{-1}. For gentamicin treatment, the decrease was nearly 70 % at 736 cm^{-1} and almost 100 % at 1320 cm^{-1}. These findings indicate the susceptibility of the bacteria to these antibiotics. For streptomycin-treated bacteria, the Raman signals remained virtually unchanged over the 180-min period, indicating the resistance of *L.innocua* to the antibiotic. It is particularly noteworthy that the SERS AST test takes only 3 h, whereas the standard tests presented above take 24 h or more. These findings highlight the efficiency of SERS-based AST and its potential to accelerate bacterial resistance detection, ultimately improving clinical decision-making.

Table 2
Results of counting zones of inhibition in disk diffusion test for the sensitivity of *L.innocua* to 3 different antibiotics: benzylpenicillin, gentamicin and streptomycin, and to AuAg@pSiNWs.

Antimicrobial agent	Diameter of inhibition zone, mm
AuAg@pSiNWs	0
Streptomycin	0
Gentamicin	7
Benzylpenicillin	15

4. Conclusions

In this study, we successfully demonstrated the use of SERS-active AuAg@pSiNWs for the antibiotic susceptibility testing of *Listeria innocua*. Scanning electron microscopy characterization revealed that the AuAg@pSiNWs have a porous structure, with Au nanoparticles catalyzing nanowire formation and a bimetallic layer coating the tops of the nanowires. The bimetallic top of the nanowires, in close proximity to the bacterial cell walls, provided an excellent SERS detection.

SERS spectra of *L. innocua* adsorbed on AuAg@pSiNWs exhibited intense and sharp Raman lines, allowing for a detailed molecular fingerprint. The observed peaks were primarily associated with bacterial cell wall constituents, such as membrane lipids, polysaccharides, proteins, Amides. The results largely matched the characteristic SERS pattern of *Listeria* species, with some peaks specific to the *L.innocua* SLCC3379 strain.

The disk diffusion test confirmed the effectiveness of benzylpenicillin and gentamicin against *L.innocua*, while streptomycin showed no inhibitory effect. SERS-based AST provided further insights, revealing a significant decrease in Raman peak intensities for *L. innocua* treated with benzylpenicillin and gentamicin, indicating bacterial susceptibility to these antibiotics. Specifically, there was an approximately 5-fold decrease at 736 cm^{-1} and nearly 100 % at 1320 cm^{-1} for benzylpenicillin, and a nearly 70 % decrease at 736 cm^{-1} and almost 100 % at 1320 cm^{-1} for gentamicin. In contrast, the Raman signals for streptomycin-treated bacteria remained virtually unchanged, confirming their resistance to this antibiotic.

It is particularly noteworthy that the SERS AST test takes only 3 h, whereas the standard tests take 24 h or more. This significant reduction in time underscores the potential of AuAg@pSiNWs substrates to expedite the AST process, providing a rapid and reliable method for bacterial

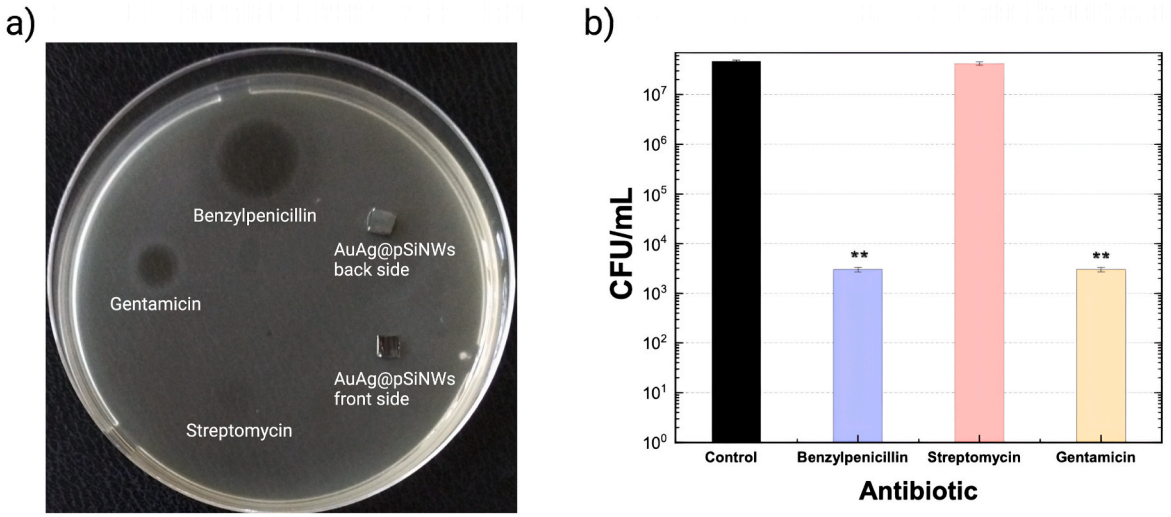

Fig. 4. Disk diffusion test for the sensitivity of *L.innocua* to 3 different antibiotics: benzylpenicillin, gentamicin and streptomycin, and to AuAg@pSiNWs (a); number of CFU/mL in control group and after the 3-h antibiotic treatment of *L.innocua* in PBS (b).

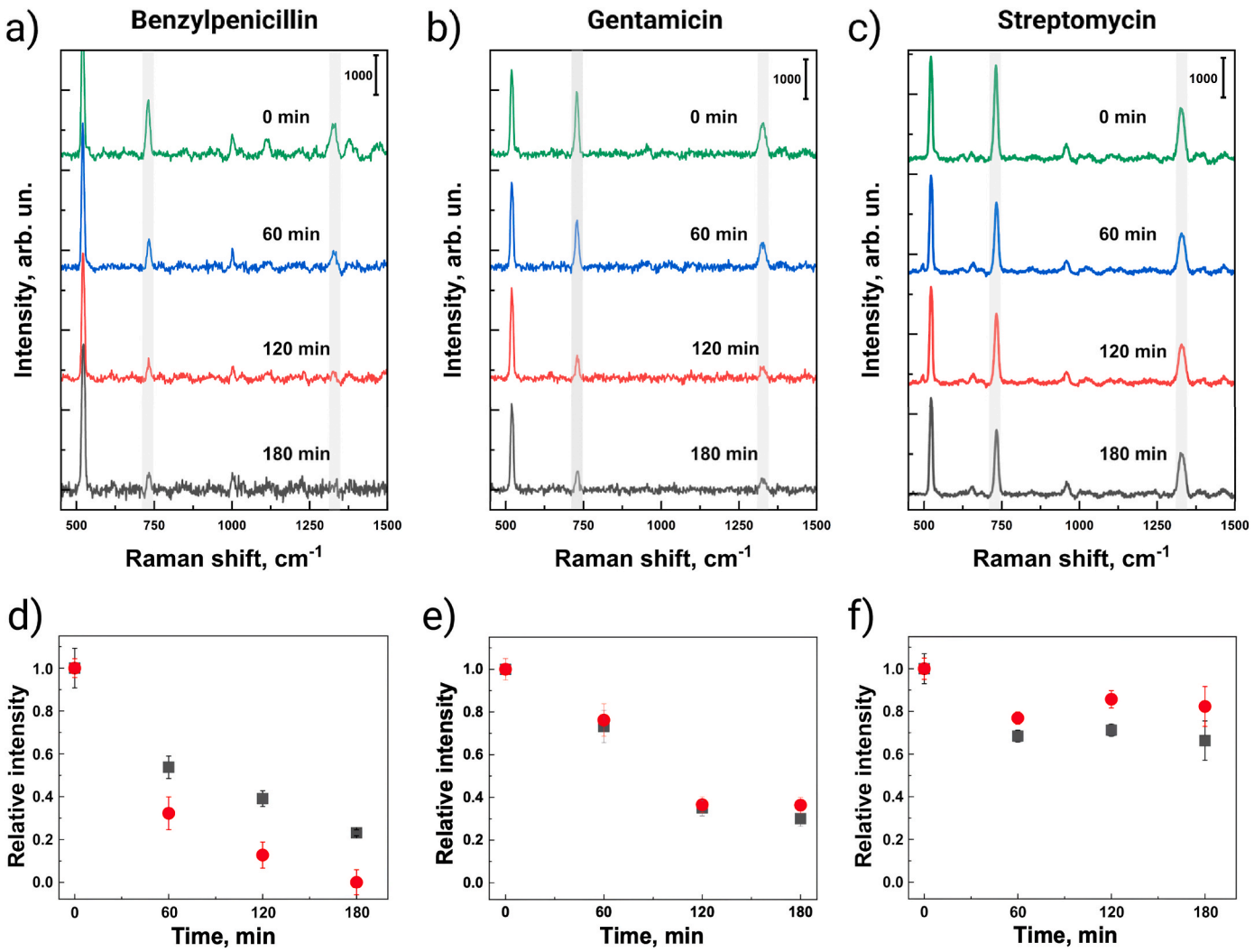

Fig. 5. AST of *L.innocua* adsorbed on SERS-active AuAg@pSiNWs towards different antibiotics: (a) benzylpenicillin, (b) gentamicin, (c) streptomycin within 3 h. Dynamics of L.*innocua* peak intensity changes at 736 cm^{-1} and 1320 cm^{-1} upon treatment with benzylpenicillin (d), gentamicin (e), streptomycin (f). The data were obtained from three independent SERS substrates, each tested with three different bacterial samples and three different samples of each antibiotic to ensure reproducibility.

detection and antibiotic susceptibility testing. This approach has potential applications in clinical diagnostics and antimicrobial resistance monitoring, offering a significant advantage in treatment of bacterial infections.

Therefore, our study demonstrates the successful application of AuAg@pSiNWs for the detection of *L. innocua*, underscoring the broader potential of this approach for bacterial diagnostics. The strong and reproducible SERS signal suggests that this platform could be extended to other clinically relevant pathogens. While different bacterial species may exhibit variations in surface composition and interaction with plasmonic nanostructures, such differences can be effectively addressed through substrate optimization or surface functionalization. Rather than limiting the significance of our findings, this aspect highlights the adaptability of the proposed method, paving the way for its application to a wider range of bacterial infections and antibiotic susceptibility testing in future studies.

CRediT authorship contribution statement

Daria A. Nazarovskaia: Writing – original draft, Investigation. **Pavel A. Domnin:** Investigation. **Oleg D. Gyuppenen:** Investigation. **Ilia I. Tsiniaikin:** Investigation. **Svetlana A. Ermolaeva:** Investigation. **Kirill A. Gonchar:** Investigation. **Liubov A. Osminkina:** Writing – review & editing, Visualization, Supervision, Investigation, Data curation, Conceptualization.

Declaration of competing interest

The authors declare the following financial interests/personal relationships which may be considered as potential competing interests: Liubov A Osminkina reports financial support was provided by Russian Science Foundation. If there are other authors, they declare that they have no known competing financial interests or personal relationships that could have appeared to influence the work reported in this paper.

Acknowledgments

This study was supported by the Russian Science Foundation (RSF), grant no. 22-72-10062. https://rscf.ru/en/project/22-72-10062/. The authors gratefully acknowledge the Microscopy and Research Facilities Sharing Center of Lomonosov Moscow State University for providing the equipment.

Appendix A. Supplementary data

Supplementary data to this article can be found online at https://doi.org/10.1016/j.rsurfi.2025.100524.

Data availability

Data will be made available on request.

References

[1] Bertagnolio, S., Dobreva, Z., Centner, C.M., Huttner, B.D., Chaillon, A., Gebreselassie, N., Wi, T., Hasso-Agopsowicz, M., 2024. WHO global research priorities for antimicrobial resistance in human health. Lancet Microbe 5, 100902. https://doi.org/10.1016/S2666-5247(24)00134-4.

[2] Henderson, A., Bursle, E., Stewart, A., Harris, P.N., Paterson, D., Chatfield, M.D., Paul, M., Dickstein, Y., Rodriguez-Baño, J., Turnidge, J.D., Kahlmeter, G., 2021. A systematic review of antimicrobial susceptibility testing as a tool in clinical trials assessing antimicrobials against infections due to Gram-negative pathogens. Clin. Microbiol. Infect. 27, 1746–1753. https://doi.org/10.1016/j.cmi.2021.03.019.

[3] Reller, L.B., Weinstein, M., Jorgensen, J.H., Ferraro, M.J., 2009. Antimicrobial susceptibility testing: a review of general principles and contemporary practices. Clin. Infect. Dis. 49 (11), 1749–1755. https://doi.org/10.1086/647952.

[4] Khan, Z.A., Siddiqui, M.F., Park, S., 2019. Current and emerging methods of antibiotic susceptibility testing. Diagnostics 9 (2), 49. https://doi.org/10.3390/diagnostics9020049.

[5] Vasala, A., Hytönen, V.P., Laitinen, O.H., 2020. Modern tools for rapid diagnostics of antimicrobial resistance. Front. Cell. Infect. Microbiol. 10, 308. https://doi.org/10.3389/fcimb.2020.00308.

[6] Rasheed, S., Kanwal, T., Ahmad, N., Fatima, B., Najam-ul-Haq, M., Hussain, D., 2024. Advances and challenges in portable optical biosensors for onsite detection and point-of-care diagnostics. TrAC Trends Anal. Chem. 173, 117640. https://doi.org/10.1016/j.trac.2024.117640.

[7] Lin, X., Zhao, M., Peng, T., Zhang, P., Shen, R., Jia, Y., 2023. Detection and discrimination of pathogenic bacteria with nanomaterials-based optical biosensors: a review. Food Chem. 426, 136578. https://doi.org/10.1016/j.foodchem.2023.136578.

[8] Dib, T., Dwivedi, A., Liu, C., Farnesi, E., Popp, J., Cialla-May, D., 2024. Surface-enhanced Raman spectroscopy in clinical point-of-care testing. In: Procházka, M., Kneipp, J., Zhao, B., Ozaki, Y. (Eds.), Surface- and Tip-Enhanced Raman Scattering Spectroscopy. Springer, Singapore. https://doi.org/10.1007/978-981-97-5818-0_17.

[9] Kneipp, K., 2007. Surface-enhanced Raman scattering. Phys. Today 60 (11), 40–46. https://doi.org/10.1063/1.2812122.

[10] Le Ru, E.C., Auguié, B., 2024. Enhancement factors: a central concept during 50 years of surface-enhanced Raman spectroscopy. ACS Nano 18 (14), 9773–9783. https://doi.org/10.1021/acsnano.4c01474.

[11] Khinevich, N., Bandarenka, H., Zavatski, S., Girel, K., Tamulevičienė, A., Tamulevičius, T., Tamulevičius, S., 2021. Porous silicon – a versatile platform for mass-production of ultrasensitive SERS-active substrates. Microporous Mesoporous Mater. 323, 111204. https://doi.org/10.1016/j.micromeso.2021.111204.

[12] Chakraborti, S., Basu, R.N., Panda, S.K., 2018. Vertically aligned silicon nanowire array decorated by Ag or Au nanoparticles as SERS substrate for bio-molecular detection. Plasmonics 13, 1057–1080. https://doi.org/10.1007/s11468-017-0605-2.

[13] Agafilushkina, S.N., Žukovskaja, O., Dyakov, S.A., Weber, K., Sivakov, V., Popp, J., Cialla-May, D., Osminkina, L.A., 2020. Raman signal enhancement tunable by gold-covered porous silicon films with different morphology. Sensors 20 (19), 5634. https://doi.org/10.3390/s20195634.

[14] Wang, M., Rachishena, P.A., Nazarovskaia, D.A., Domnin, P.A., Tsiniaikin, I.Y.I., Efimova, A.I., Ermolaeva, S.A., Osminkina, L.A., Gonchar, K.A., 2024. Diagnostics of Escherichia coli using Fabry–Perot interference in silicon nanostructures of various morphologies. J. Sib. Fed. Univ. Math. Phys. 17 (6), 798–807.

[15] Soler, M., Belushkin, A., Cavallini, A., Kebbi-Beghdadi, C., Greub, G., Altug, H., 2017. Multiplexed nanoplasmonic biosensor for one-step simultaneous detection of Chlamydia trachomatis and Neisseria gonorrhoeae in urine. Biosens. Bioelectron. 94, 560–567. https://doi.org/10.1016/j.bios.2017.03.047.

[16] Muthukumar, D., Shtenberg, G., 2023. SERS-based immunosensor for E. coli contaminants detection in milk using silver-coated nanoporous silicon substrates. Talanta 254, 124132. https://doi.org/10.1016/j.talanta.2022.124132.

[17] Muthukumar, D., Shtenberg, G., 2024. Quantitative detection of Staphylococcus aureus using aptamer-based bioassay coupled with porous Si SERS platform. J. Sci. Adv. Mater. Devices, 100690. https://doi.org/10.1016/j.jsamd.2024.100690.

[18] Das, S., Saxena, K., Tinguely, J.C., Pal, A., Wickramasinghe, N.L., Khezri, A., Vishesh Dubey, V., Ahmad, A., Perumal, V., Ahmad, R., Wadduwage, D.N., Ahluwalia, B.S., Mehta, D.S., 2023. SERS nanowire chip and machine learning-enabled classification of wild-type and antibiotic-resistant bacteria at species and strain levels. ACS Appl. Mater. Interfaces 15 (20), 24047–24058. https://doi.org/10.1021/acsami.3c00612.

[19] Jabbar, A.A., Alwan, A.M., Zayer, M.Q., Bohan, A.J., 2020. Efficient single cell monitoring of pathogenic bacteria using bimetallic nanostructures embedded in gradient porous silicon. Mater. Chem. Phys. 241, 122359. https://doi.org/10.1016/j.matchemphys.2019.122359.

[20] Žukovskaja, O., Agafilushkina, S., Sivakov, V., Weber, K., Cialla-May, D., Osminkina, L., Popp, J., 2019. Rapid detection of the bacterial biomarker pyocyanin in artificial sputum using a SERS-active silicon nanowire matrix covered by bimetallic noble metal nanoparticles. Talanta 202, 171–177. https://doi.org/10.1016/j.talanta.2019.04.047.

[21] Kartashova, A.D., Gonchar, K.A., Chermoshentsev, D.A., Alekseeva, E.A., Gongalsky, M.B., Bozhev, I.V., Eliseev, A.A., Dyakov, S.A., Samsonova, J.V., Osminkina, L.A., 2022. Surface-enhanced Raman scattering-active gold-decorated silicon nanowire substrates for label-free detection of bilirubin. ACS Biomater. Sci. Eng. 8 (10), 4175–4184. https://doi.org/10.1021/acsbiomaterials.1c00728.

[22] Gonchar, K.A., Alekseeva, E.A., Gyuppenen, O.D., Bozhev, I.V., Kalinin, E.V., Ermolaeva, S.A., Osminkina, L.A., 2022. Optical express monitoring of internalin B protein of Listeria monocytogenes pathogenic bacteria using SERS-active silver-decorated silicon nanowires. Opt. Spectrosc. 130 (9), 521–526. https://doi.org/10.1134/S0030400X22110017.

[23] Nazarovskaia, D.A., Domnin, P.A., Gyuppenen, O.D., Tsiniaikin, I.I., Ermolaeva, S. A., Gonchar, K.A., Osminkina, L.A., 2023. Advanced bacterial detection with SERS-active gold-and silver-coated porous silicon nanowires. Bull. Russ. Acad. Sci. Phys. 87 (1), 41–46. https://doi.org/10.1134/S1062873823704385.

[24] Massad-Ivanir, N., Shtenberg, G., Raz, N., Gazenbeek, C., Budding, D., Bos, M.P., Segal, E., 2016. Porous silicon-based biosensors: towards real-time optical detection of target bacteria in the food industry. Sci. Rep. 6 (1), 38099. https://doi.org/10.1038/srep38099.

[25] Parker Jr., J.H., Feldman, D.W., Ashkin, M., 1967. Raman scattering by silicon and germanium. Phys. Rev. 155 (3), 712. https://doi.org/10.1103/PhysRev.155.712.

[26] Uusitalo, S., Kögler, M., Välimaa, A.L., Popov, A., Ryabchikov, Y., Kontturi, V., Siitonen, S., Petäjä, J., Virtanen, T., Laitinen, R., Kinnunen, M., Meglinski, I., Kabashin, A., Bunker, A., Viitalab, T., Hiltunen, J., 2016. Detection of Listeria innocua on roll-to-roll produced SERS substrates with gold nanoparticles. RSC Adv. 6 (67), 62981–62989. https://doi.org/10.1039/c6ra08313g.

[27] Tzeng, Y., Lin, B.Y., 2020. Silver SERS adenine sensors with a very low detection limit. Biosensors 10 (5), 53. https://doi.org/10.3390/bios10050053.

[28] Sundaram, J., Park, B., Kwon, Y., Lawrence, K.C., 2013. Surface enhanced Raman scattering (SERS) with biopolymer encapsulated silver nanosubstrates for rapid detection of foodborne pathogens. Int. J. Food Microbiol. 167 (1), 67–73. https://doi.org/10.1016/j.ijfoodmicro.2013.05.013.

[29] Cheng, S., Tu, Z., Zheng, S., Cheng, X., Han, H., Wang, C., Xiao, R., Gu, B., 2021. An efficient SERS platform for the ultrasensitive detection of Staphylococcus aureus and Listeria monocytogenes via wheat germ agglutinin-modified magnetic SERS substrate and streptavidin/aptamer co-functionalized SERS tags. Anal. Chim. Acta 1187, 339155. https://doi.org/10.1016/j.aca.2021.339155.

[30] Busch, R.T., Karim, F., Sun, Y., Fry, H.C., Liu, Y., Zhao, C., Vasquez, E.S., 2021. Detection and aggregation of Listeria monocytogenes using polyclonal antibody gold-coated magnetic nanoshells surface-enhanced Raman spectroscopy substrates. Front. Nanotechnol. 3, 653744. https://doi.org/10.3389/fnano.2021.653744.

[31] Witkowska, E., Korsak, D., Kowalska, A., Księżopolska-Gocalska, M., Niedziółka-Jönsson, J., Roźniecka, E., Michałowicz, W., Albrycht, P., Podrażka, M., Hołyst, R., Waluk, J., Kamińska, A., 2017. Surface-enhanced Raman spectroscopy introduced into the International Standard Organization (ISO) regulations as an alternative method for detection and identification of pathogens in the food industry. Anal. Bioanal. Chem. 409, 1555–1567. https://doi.org/10.1007/s00216-016-0090-z.

[32] Wang, W., Hynninen, V., Qiu, L., Zhang, A., Lemma, T., Zhang, N., Ge, H., Toppari, J.J., Hytönen, V.P., Wang, J., 2017. Synergistic enhancement via plasmonic nanoplate-bacteria-nanorod supercrystals for highly efficient SERS sensing of food-borne bacteria. Sens. Actuator. B Chem. 239, 515–525. https://doi.org/10.1016/j.snb.2016.08.040.